Local Dynamics and Primitive Path Analysis for a Model Polymer Melt near a Surface

Mihail Vladkov* and Jean-Louis Barrat

Laboratoire de Physique de la Matière Condensée et Nanostructures Université Lyon 1, CNRS, UMR 5586 Domaine Scientifique de la Doua F-69622 Villeurbanne Cedex, France

Received November 12, 2006; Revised Manuscript Received March 20, 2007

ABSTRACT: Using molecular dynamics simulations, we apply primitive path and local Rouse modes analysis to study the chain conformations and the local dynamics and viscosity of a model polymer melt near a flat wall and a wall presenting some bonding sites. The presence of the flat wall leads to acceleration of the dynamics both for unentangled and weakly entangled melts and to a depletion in the entanglement density in the vicinity of the wall. When the surface bears grafted chains, we show that the melt chains are accelerated in the unentangled regime and slowed down in the entangled regime. By analyzing the primitive paths, we show that the observed slowing down in presence of grafted chains is due to an increase in the entanglement density in the interfacial layer. In contrast, for a bare surface we observe a depletion of the entanglements at the interface. The presence of a relatively small density of grafting sites leads to a reinforcement of the entanglement network locally increasing the entanglement density.

I. Introduction

Nanocomposite polymer based materials have many interesting properties leading to their extensive usage in practical applications. It has been long known that adding filler particles to a polymer melt can lead to substantial modifications in its mechanical properties. The properties of polymer−filler composites are often associated with filler clustering and percolation[1,2] but several studies over the past several years showed that the effect is also observable below the percolation threshold.[3,4] This indicates that the particle−matrix interface is another crucial ingredient in the complex physics of filled elastomers. Another indication of the importance of surface effects lies in the fact that small size particles (nanoparticles) have a much greater effect compared to micrometer size fillers. The nature of the polymer filler interactions was shown to be very important. It was established by experiment[5] and simulation[6] that attractive interactions lead to an increase of the glass transition temperature near the interface. With this argument reinforcement can be partly explained by formation of "harder", glassy layers with slow dynamics around attractive fillers. Yet this explanation is not sufficient as reinforcement (a lower value, but still nearly 100%) was experimentally measured in nanocomposites at temperatures twice as high as the glass transition temperature of the matrix.[3] Most of the fillers used in practical applications (tires) and leading to substantial reinforcement, such as treated silica particles, exhibit a globally repulsive interface with some sites that can covalently bond polymer chains from the melt. The microscale physics of interfacial reinforcement remain unclear in this case. Experimental studies[3] suggested that chain entanglements in the vicinity of the surface should play a major role in the reinforcement which can be explained by the presence of trapped entanglements near the interface. Theoretical studies have qualitatively suggested that the density of entanglements decreases in the vicinity of a wall[8,9] because of the average decrease in chain dimensions established earlier by simulation.[11,12] On the experimental side the validity of this assumption was recently questioned for free-standing films,[7] but clear evidence of this phenomenon near a wall is still lacking, and it could not be related to mechanical properties.

Recent advances in molecular simulation has made possible a precise study of these problems. The well-established concept of entanglement in a polymer melt can be "observed" by direct primitive path analysis.[13,14] We recently developed an equilibrium method for studying the mechanical properties of a melt that can be used to assess local viscoelastic properties.[15] Using these methods we analyze the dynamics and the entanglement density of a polymer melt near a flat wall with or without bonding sites and give a generic explanation of the melt slowing down or acceleration at the interface as a function of molecular weight.

The systems under study are briefly described in the next section. We then discuss the local dynamics of the melt in terms of the Rouse modes of the chains for unentangled and weakly entangled melts. Finally, we study the structure of primitive paths in the vicinity of the wall, in order to explain the observed dynamical behavior.

II. System Description and Methods

A. Model. The chains are modeled by an abstract and generic, though well studied, bead spring model—the rather common "Lennard-Jones + FENE".[16] All monomers in the system interact via the Lennard-Jones potential:

$$U_{\mathrm{lj}}(r) = \begin{cases} 4\epsilon((\sigma/r)^{12} - (\sigma/r)^{6}), & r \le r_{\mathrm{c}} \\ 0, & r > r_{\mathrm{c}} \end{cases} \qquad (1)$$

where $r_c = 2.5\sigma$. Neighboring monomers in the same chain are linked by the FENE (Finite extension nonlinear elastic) potential:

$$U_{\mathrm{FENE}}(r) = -\frac{k}{2}R_0^{\,2}\ln\left(1 - \left(\frac{r}{R_0}\right)^2\right), \; r < R_0 \qquad (2)$$

where $R_0 = 1.5\sigma$ and $k = 30.0\epsilon/\sigma^2$.

The temperature of the melt was fixed in all simulations at $k_{\mathrm{B}}T = \epsilon$, well above the glass transition temperature for our

* To whom correspondence should be addressed. E-mail: mihail.vladkov@lpmcn.univ-lyon1.fr.

10.1021/ma062607r CCC: $37.00
Published on Web 04/19/2007

model ($k_BT_g \sim 0.42\epsilon$). We studied systems of chain length of 10, 20, 50, 100, and 200 beads with a total number of beads ranging from 6400 to 110000. This allows us to investigate the crossover into the weakly entangled regime, with an entanglement length N_e estimated for this model in the vicinity of 65.[13] The melt was confined between walls in the z direction with $L_z > 5R_g$ in all cases. The interaction between the wall and the beads consists of an integrated 9−3 Lennard-Jones short range potential. Its parameters were chosen to crudely reproduce the PE−silica interaction. The bead diameter was mapped through the polymer C_∞ ratio[17] to give $\sigma \sim 8$ Å. We apply a mixing rule using values for the PE and silica interaction intensity found in the literature[18] to obtain for the wall potential $\sigma_{wall} = 0.6875\sigma$ and $\epsilon_{wall} = 0.82\epsilon$. The potential is cut off at $2^{1/6}\sigma_{wall} = 0.77\sigma$ and shifted. It has a repulsive part ($|z - z_w| \leq 0.59\sigma$) and a short range attraction ($0.59\sigma < |z - z_w| \leq 0.77\sigma$). The potential well depth seen by the particles is thus 0.3ϵ, much smaller than $k_BT = 1\epsilon$ so that the attraction is very weak. The wall is represented either by the flat wall potential only or by a 111 surface of an fcc lattice made of spherical particles, supplemented by the same flat potential in the second layer to prevent beads from escaping. For each chain length, two systems were prepared: one with a flat wall and one with chemisorbing sites on the wall, where chains are anchored. We refer to the chains chemically attached to the surface as "grafted". The chemical bonds are not associated with specific chain sites (as in end grafted polymers) so the attached chains can also be described as irreversibly adsorbed. Silica surface treatment consists in introducing very short chain molecules on the surface that covalently bond with some sites on the surface on one side and with monomers on the other side. The number of bonding sites in the simulation was calculated assuming that 4% of the silica molecules covering the surface of the wall are active and react with the bonding molecule, this number being chosen to reflect experimental situations.[18] The surface density of active sites is therefore $0.2\sigma^{-2}$. The resulting bond between a wall particle and a coarse grained bead is thus a soft entropic spring of finite length on the order of several chemical units that is modeled by a non-harmonic spring:

$$U_{bond} = \frac{\epsilon_{bond}(r - r_0)^2}{[\lambda^2 - (r - r_0)^2]} \quad (3)$$

The spring constant was set to $\epsilon_{bond} = (3/2)k_BT = 1.5\epsilon$, the equilibrium distance and the finite extension length are set to $r_0 = \lambda = 0.8\sigma$. These parameters define a soft spring freely fluctuating with ambient temperature that cannot extend further than 1.6σ away from the surface. The time step in the simulation runs was set to 0.005τ. All the simulations were performed using the LAMMPS code.[22]

B. System Preparation and Static Properties. At first a pure polymer melt was confined at a given pressure ($0 \leq P \leq 0.8$ depending on the system) between two walls. Pressure is monitored by calculating the normal force on the walls. Then, in order to obtain the system with grafted chains from this initial configuration, a new bond is created between each active wall site and the closest monomer of the melt. Only one bond per active wall site is allowed while a monomer can be bonded to several wall atoms as it is a coarse-grained bead representing several chemical units (1 bead $\sim 6CH_2$). There is no preferential bonding for end or middle monomers, matching the physical situation of polymers bonding to silica beads. The new system is now equilibrated at the same pressure as the original system, its pressure being calculated via the force on the wall and the grafted chains. All systems were equilibrated for $5 \times 10^3\tau$ ($N = 10$) to $5 \times 10^4\tau$ ($N = 100$) and $4 \times 10^5\tau$ ($N = 200$) before production runs of about $10^5\tau$. The equilibration time is in all cases larger than twice the longest polymer relaxation time. For chain lengths smaller than 200 we study both dynamics and primitive paths, for the $N = 200$ systems we perform only primitive path analysis due to the high computational cost for simulating such large systems and the long runs needed to measure relaxation times accurately. The grafting procedure creates a population of grafted chains near the wall having around 3.5 grafted beads per chain (Figure 1). The grafted chains extend in all systems a distance of maximum $2.5R_G$ in the melt (Figure 2). There are no bridges between the walls.

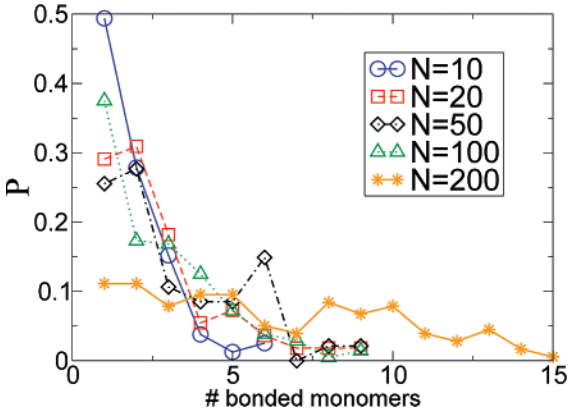

Figure 1. Distribution of the number of bonded monomers per grafted chain in the systems with treated surface

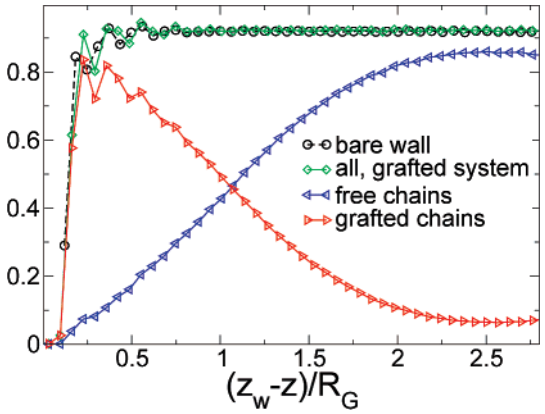

Figure 2. Monomer density profile of the system with and without grafted chains for $N = 100$. The densities of the monomers of the grafted and the free chains are also shown. The density profiles in the other systems have similar behavior.

We start with a brief study the influence of the surface in the two configurations on the static properties of the chains. The z component of the mean end to end vector and the radius of gyration of the chains decreases in the vicinity of the wall and there is a very slight increase in the size of the chains parallel to the wall (see Figure 3). The effects are observed to extent within about one to two R_G (bulk value) from the wall, as was established in earlier simulations.[11,12]

In systems with grafted chains the decrease is slightly more pronounced and extends farther into the melt, up to $2R_G$ from the wall surface. This slightly larger length scale is close to the typical spatial extension of the grafted chains, which are on average more extended than the bulk chains.

III. Local Dynamics of Polymer Chains

A. Desorption and Mean-Square Displacement. We can get a qualitative idea of the melt dynamics in the bulk and near

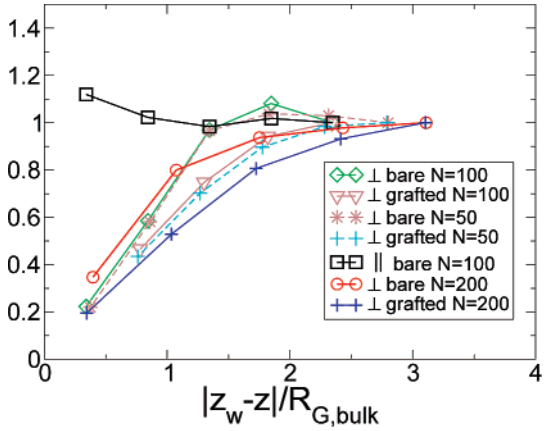

Figure 3. Variation of the perpendicular component of the radius of gyration squared, as a function of the distance to the wall divided by the bulk R_G. The results are normalized by the bulk value $\langle R_G^2 \rangle$. The parallel component is shown for $N = 100$, the other systems having similar behavior.

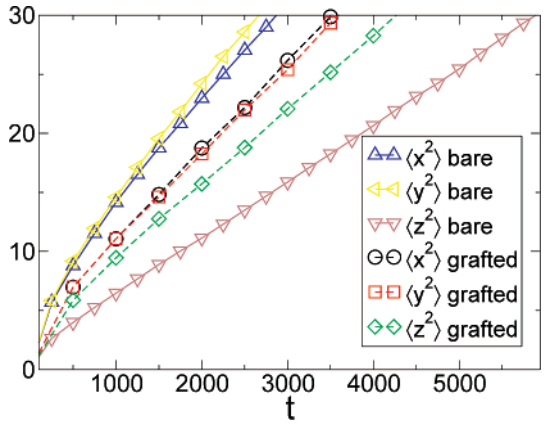

Figure 4. Monomer mean-square displacement in the vicinity of the wall for the system $N = 20$ with and without grafted chains. The direction perpendicular to the surface is z.

the surface by looking at the local mean-square displacement of the polymer chains. We define the bulk and surface chains mean-square displacement by

$$\langle R^2(\tau)\rangle_{\text{bulk}} = \frac{1}{TN_{\text{ch}}^z}\int \mathrm{d}t \sum_{i;-\sigma<Z_{\text{cm}}^i(t)<\sigma} (R_i(t+\tau) - R_i(t))^2 \quad (4)$$

$$\langle R^2(\tau)\rangle_{\text{wall}} = \frac{1}{TN_{\text{ch}}^z}\int \mathrm{d}t \sum_{i;z_w-2\sigma<|Z_{\text{cm}}^i(t)|<z_w} (R_i(t+\tau) - R_i(t))^2 \quad (5)$$

In the case of a bare surface we find that surface chains have increased mobility parallel to the surface in the x and y direction compared to bulk chains and they are slowed down perpendicular to the surface. For a wall with grafted chains the free chains in the vicinity of the wall are slower in the parallel direction (Figure 4)—this is attributed to the presence of the grafted chains acting as obstacles for motion parallel to the wall.

A more surprising result is that, in the presence of grafted chains, the free chains are faster than the chains near a bare wall in the perpendicular direction (Figure 4). This kind of behavior can be understood considering the desorption mechanism from a flat surface.[19] We know that for a flat wall, surface chains having many monomers on the surface are very slow to desorb and are thus responsible for a slowing down in dynamics near the surface. This is seen in the perpendicular slowing down in the bare wall system. In the presence of grafted chains, there are fewer free chains near the surface, as the corresponding conformations are achieved by the grafted chains that do not desorb. The presence of grafted chains makes the surface rough on a scale comparable to the polymer size, it can be argued that adsorption and desorption on a rough surface for polymers is faster as it involves less entropy loss than in the case of a flat wall.[20] Thus, the free chains population near the surface has faster exchange dynamics with the bulk chains.

B. Rouse Modes. We study the local dynamics of the polymer chains by monitoring the relaxation of the Rouse modes of the chains:

$$X_p(t) = \frac{1}{N}\sum_{n=1}^{N} r_n(t)\cos\left(\frac{(n-1/2)p\pi}{N}\right),\ p = 0, \ldots, N-1 \quad (6)$$

with N the chain length and $r_n(t)$—the position of the nth monomer in the chain at the time t. The correlation of the pth Rouse mode describes the relaxation of a subchain of N/p monomers, so that the study of this single chain quantity allows to probe the dynamics on different length scales. Being a local single chain quantity, the correlation of the Rouse modes allows us to investigate the dynamics in different sub-volumes of a non-homogeneous system, provided they contain a large enough number of chains. It is also a route to estimate the local viscosity in each region, as discussed in ref 15. In our confined systems, we define the local modes' relaxation as a function of the z coordinate as

$$\langle X(\tau)X(0)\rangle(z) = \frac{1}{TN_{\text{ch}}^z}\int \mathrm{d}t \sum_{i;z-\mathrm{d}z<Z_{\text{cm}}^i(t)<z+\mathrm{d}z} X_i(t+\tau)X_i(t) \quad (7)$$

It is expected that the slowest Rouse mode relaxes on a time scale smaller than the time needed for a chain to diffuse its own size. Hence, we choose a slice width on the order of R_G, so that the center of mass of a chain stays (statistically) within the same slice while the correlation is measured. This allows us to access local dynamics with a spatial resolution on the order of R_G, which is better than the resolution associated with measurements of the mean-square displacement. For the systems with grafted chains we define relaxation times by considering *only the modes of the free chains*. Hence the values of the relaxation times shown in this study are not affected directly by the frozen dynamics of the tethered chains. Our goal is to understand the influence of the presence of the grafted chains on the remaining melt and to capture, if any, matrix mediated slowing down.

We estimate the Rouse times by an exponential fit of the normalized correlation function of the first mode, which have in all cases a clear exponential behavior. We estimate separately the relaxation of chain conformations following the three directions in order to take into account the spatial inhomogeneity near the surface. For chain lengths of $N = 10$ and $N = 20$, we observe a clear decrease in the relaxation times of the modes near the wall in all systems, regardless of the presence of grafted chains (Figure 5). In the case of a flat surface, this acceleration is expected and can be understood in terms of reduction of the monomeric friction due to the repulsion of the surface.[6] We also studied the influence of the pressure and the microscopic wall roughness on the acceleration of the chains. They were found to have a negligible effect on the modes relaxation times in the melt. Cage effects associated with microscopic roughness of the wall are relatively unimportant for chain molecules

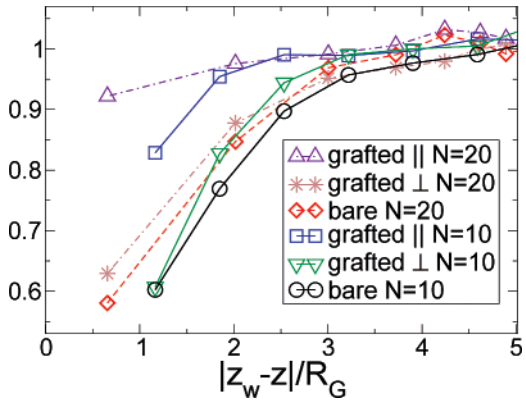

Figure 5. Local Rouse times normalized by the bulk value for chain lengths of 10 and 20 and for the free chains in the systems with grafted chains (referred to as "grafted") and for the chains in the system without grafted chains (referred to as "bare").

compared to simple fluids, due to the competition with bond constraints associated with the neighboring monomers in the chain.

As the grafted chains act as soft obstacles for the free chains one could expect that the free chains will be slower close to the wall than in the bulk. Studying the local Rouse times, we find that this assumption is not true for melts with chain lengths $N = 10$, 20. In the systems where there are grafted chains on the surface, the free chains in the immediate vicinity of the wall are still accelerated with respect to the bulk chains. The effect of the grafted chains is seen when comparing the systems with and without grafted chains. In the direction parallel to the surface the free chains in the immediate vicinity of the wall having grafted chains are about 20% ($N = 10$) and 30% ($N = 20$) slower compared to the chains seeing a bare surface, but they are still accelerated by 20% ($N = 10$) and 10% ($N = 20$) compared to the bulk dynamics (see Figure 5). In the perpendicular direction the chain conformations equilibrate in about the same time for the two types of systems. For these systems of short chains, the slowing down due to the grafted chains is not sufficient to overcome the acceleration due to the surface and we do not expect reinforcement with respect to the bulk properties of the material, as discussed in the next section.

For chain lengths $N > 20$ we measure the modes' relaxation times as the integral of the normalized correlation function so that an exponential behavior of the latter is not required. Although the relaxation is not strictly exponential, the resulting values are close to those that would be obtained using an exponential fit. For chain lengths around and above the entanglement length we observe an acceleration for the first Rouse mode in the case of a bare wall, very similar to the case of short chains. The influence of grafted chains, however, is much more important than for short chains. In the systems with grafted chains of $N = 50$ 100, we measure a slowing down for the largest relaxation time in the parallel direction (of around 10% for $N = 50$ and 40% for $N = 100$ within a distance of R_G from the wall) with respect to the dynamics in the middle of the film (see Figure 6). The average relaxation times in the layer feeling the presence of the grafted chains are larger than those for the system without grafted chains. On average, for $N = 100$, the mean relaxation times of the first five Rouse modes are increased by ~20% in the presence of grafted chains, compared to what is observed for a bare wall (see Figure 7). In summary, the presence of grafted chains induces a slowing down for all modes (compared to the bare wall case), and in the case of the first mode a slowing down compared to the bulk is also observed.

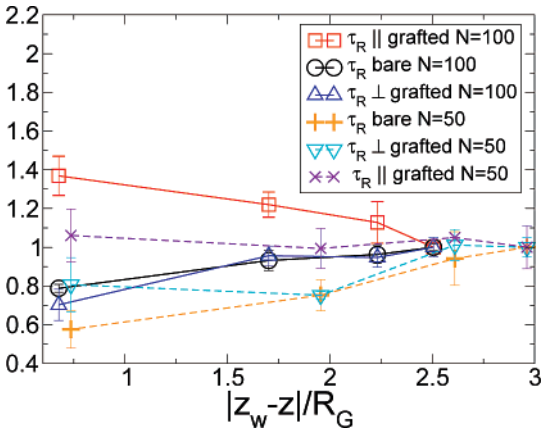

Figure 6. Local Rouse times (first mode), normalized by the bulk value, for chain lengths of 50 and 100 and systems with and without grafted chains.

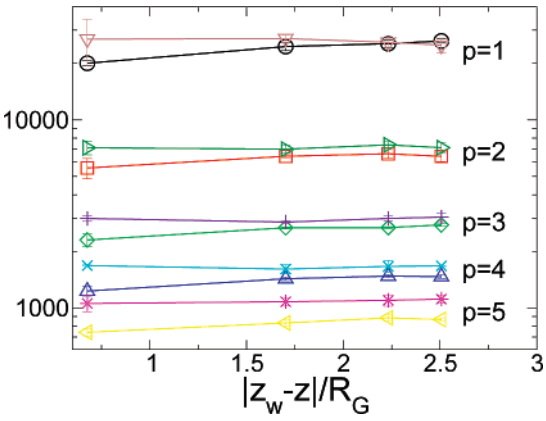

Figure 7. Local relaxation times of the first five Rouse modes for chain length of 100 for the systems with and without grafted chains. The system without grafted chains is systematically the faster one. Bare wall: $p = 1$, circles; $p = 2$, rectangles; $p = 3$, diamonds; $p = 4$, triangles; $p = 5$, left triangles. Grafted: $p = 1$, down triangles; $p = 2$, right triangles; $p = 3$, pluses; $p = 4$, crosses; $p = 5$, stars.

In the z direction the conformation dynamics for systems both with and wothout grafted chains vary similarly as a function of distance to the surface.

In the following, we argue that the substantial slowing down observed in the relaxation time of the first mode is due to entanglement effects near the surface. If the slowing down is due to entanglements, we should still have faster dynamics close to the surface for chain segments well below the entanglement threshold. In other words, the relaxation of a mode p such that $N/p > N_e$ should be slowed down when approaching the wall, while the dynamics of a mode p satisfying $N/p < N_e$ should be similar to the unentangled case, i.e., accelerated with respect to its value in the middle of the film. This assumption is confirmed by the measurement of the relaxation of higher Rouse modes of the chains (see Figure 8). In terms of effective monomeric friction the presence of the surface still leads to relative acceleration of the dynamics in the immediate vicinity of the wall on length scales smaller than the tube diameter (as in the case of unentangled chains). This leads to a relative acceleration of the small scale modes in the interface layer when approaching the wall. On the scale of entanglements the shorter the distance to the wall is, the slower are the dynamics. This issue will be further investigated in terms of entanglements in the next section.

In summary, the presence of a flat poorly adsorbing surface results in the formation of an interfacial layer where the dynamics and chain conformations are different from the bulk.

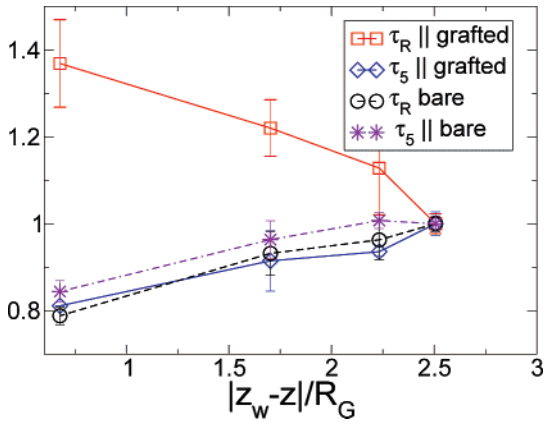

Figure 8. Relative variation of local relaxation times normalized ($N = 100$) by the bulk value. The first (entangled) mode and the fifth mode for the free chains in the system with grafted chains and the chains near a bare surface are shown. All modes except the first mode in the grafted system follow the same qualitative behavior and are accelerated close to the surface. The first mode of the free chains in presence of grafted chains is slowed down.

Chains tend to lie flat on the surface so that their dimension perpendicular to the surface is reduced in a layer extending one to two gyration radii from the surface. The presence of the surface also alters the dynamical properties of the melt in its vicinity within around two to three bulk R_G. The presence of grafted chains on the surface increases the thickness of the interfacial layer as far as static properties are concerned due to the tendency of the grafted chains to have an extension larger than the bulk R_G.

In the unentangled regime, the presence of a flat poorly adsorbing surface results in a relative acceleration of the melt dynamics when approaching the wall regardless of the presence of grafted chains on the surface. The presence of grafted chains slows down the free chains dynamics parallel to the surface compared to the system without grafted chains but chains are accelerated with respect to the bulk.

The situation changes when the chain length increases and we enter the entangled regime. In the case of entangled melts, the relaxation of entangled modes p such that $N/p > N_e$ is slowed down compared to the bulk near the surface in presence of grafted chains. In the next section we will relate this to the local entanglement density. The local dynamics at length scales shorter than the entanglement length is slower with grafted chains than without, but remains accelerated close to the surface with respect to the bulk.

In the perpendicular direction adsorption−desorption dynamics are slightly accelerated compared to the system without grafted chains. This is due to the fact that the slowest chains in the vicinity of a flat wall tend to be those with most contacts with the wall.[19] In the grafting process, these chains are removed from the population of "free" chains that we consider here.

C. Local Stress Relaxation Function. Next we calculate the local stress relaxation in our systems using the method discussed in ref 15. Each mode p of the chains has a contribution to the stress auto correlation function:

$$G_p(t) = \frac{\rho k_B T}{N} \frac{\langle X_{p\alpha}(t) X_{p\beta}(t) X_{p\alpha}(0) X_{p\beta}(0)\rangle}{((\langle X_{p\alpha}^2\rangle + \langle X_{p\beta}^2\rangle)/2)^2} \tag{8}$$

where $\alpha, \beta = x, y, z$. Here we calculate these quantities locally in slices parallel to the wall as for the Rouse modes in the previous section:

$$\langle X_{p\alpha}(t) X_{p\beta}(t) X_{p\alpha}(0) X_{p\beta}(0)\rangle(z) \tag{9}$$

$$= \frac{1}{TN_{ch}^z} \int ds \sum_{i; z-dz<Z_{cm}^i(t)<z+dz} X_{p\alpha}^i(s+t)\, X_{p\beta}^i(s+t)\, X_{p\alpha}^i(s) X_{p\beta}^i(s) \tag{10}$$

$$\langle X_{p\alpha}^2\rangle(z) = \frac{1}{TN_{ch}^z} \int ds \sum_{i; z-dz<Z_{cm}^i(t)<z+dz} (X_{p\alpha}^i(s))^2 \tag{11}$$

The contribution to the viscosity of the mode is $\eta_p = \int_0^\infty G_p(t)\, dt$ and the total viscosity is given by $\eta = \eta_{p=1} + ... + \eta_{p=N-1}$. For chain lengths of $N = 10$ and $N = 20$ the integral of the stress correlation function is estimated from all the Rouse modes and for chains of $N = 50$ and $N = 100$ only the first ten modes were considered. The contribution of the 11th mode for $N \geq 50$ was found to be less than 1% of the contribution of the first mode. The contribution of the non-polymeric stress (associated with short range interactions between monomers rather than with chain connectivity) on very short time scales was neglected. While this leads to an underestimate of the stress relaxation on the order of 20% in the unentangled regime, this contribution is negligible (< 1%) for longer chains as discussed in.[15] The average local integrated value of G_{local} is shown in Figure 9. For chains of length $N = 100$, the grafting induces an increase in the integrated stress relaxation function in a range of around $2R_G$ from the wall, as could be expected from the increase in the relaxation times, due to the increased entanglement density. A smaller increase in a layer of R_G is observed for the chains around the entanglement threshold ($N = 50$). For unentangled melts, there is essentially no difference between the results with and without grafted chains.

IV. Primitive Path Analysis

In order to interpret the slowing down in the dynamics for entangled systems in the presence of grafted chains, we perform a local primitive path analysis following the algorithm discussed in ref 14. Starting from independent initial states separated by more than a chain relaxation time, the chain ends are kept fixed, while the intrachain pair interactions are switched off and the equilibrium bond length is reduced to zero while increasing the bond tension to $k = 100\epsilon/\sigma^2$. In the systems with grafted chains the grafting bonds are maintained, the primitive path quench is applied to all the chains and the parameters of the primitive paths are measured for the free chains only as in the previous section. We measure locally, as a function of the distance to the surface, the length of the primitive paths (L_{pp}). If no entanglements exist between the chains the length of their primitive paths should be equal or very close to their end-to-end distance. The presence of entanglements leads to primitive paths longer than the end-to-end distance with a typical Kuhn length $a_{pp} = \langle R^2\rangle/L_{pp}$ and an average bond length $b_{pp} = L_{pp}/N$, which are related to the entanglement length.[13] We can define the number of monomers in straight primitive path segments by

$$N_{pp}(N) = \frac{a_{pp}}{b_{pp}} = \frac{N\langle R^2\rangle}{L_{pp}^2} \tag{12}$$

For short chains with no entanglements at all, as their primitive path length equals their end to end distance, eq 12 gives $N_{pp} = N$. When the chain length becomes comparable to the entanglement length we are in a transition state (around one entanglement per chain) and the result of 12 is $N_{pp} < N_e$, smaller than the real value of the entanglement length. For longer chains ($N >$

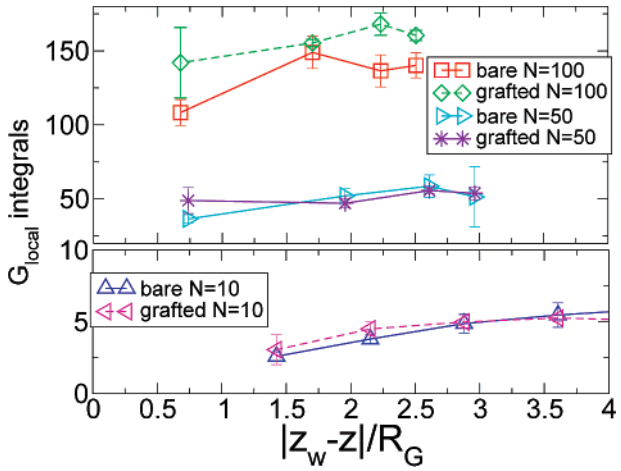

Figure 9. Local integral of $G(t)$ for the different systems. The values are calculated as the mean of the three components xy, xz, and yz of the stress correlation function integral and error bars indicate the dispersion around the mean value.

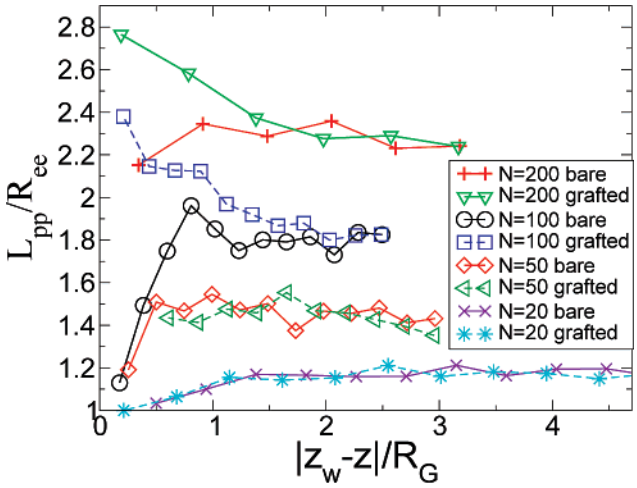

Figure 10. Local ratio of the primitive path length to the end-to-end chain distance in the different systems. This ratio for a given chain is proportional to its number of entanglements.

$2N_e$) with several entanglements per chain we have $N_{pp}(N) = N_e$. The statistical determination of N_e via eq 12 is already accurate and the result no longer depends on the chain length. The average number of entanglements per chain is $(L_{pp}/a_{pp}) - 1$. For chain lengths of 10 and 20 the primitive path analysis shows that we are in the unentangled regime as expected (with 0.1 entanglements per chain for $N = 20$). For $N = 50$ the melt is closer but still under the entanglement threshold with 0.5 entanglements per chain. For a chain length of 100 there are 1.1 entanglements per chain, the system is weakly entangled and for $N = 200$ we measure on average 2.2 entanglements per chain. As expected in the unentangled case (Figure 10), the behavior in terms of primitive paths of the free chains in the system with and without grafted chains is identical. There is a slight decrease of the primitive path length close to the surface that is related to the decrease in the dimensions of chains lying flat on the surface. A noticeable difference is seen in the entangled case where the ratio L_{pp}/R_{ee} becomes larger for the free chains near the surface bearing tethered chains, while it decreases with respect to the bulk value for the bare wall system.

Measuring separately the primitive path length and the end-to-end distance in the systems of $N = 100$ 200 (see Figure 11 and 12) we see that in the presence of grafted chains on the surface the length of the primitive paths of the free chains

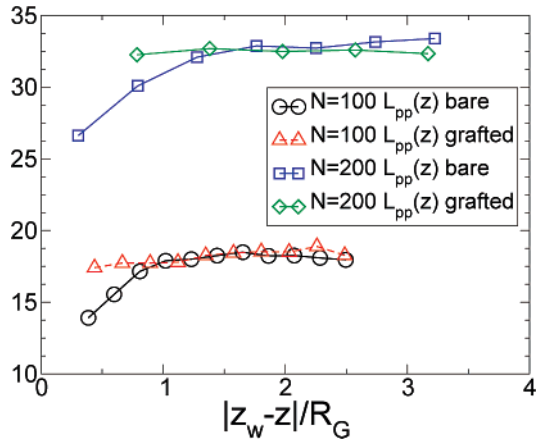

Figure 11. Local primitive path length for $N = 100$ and 200.

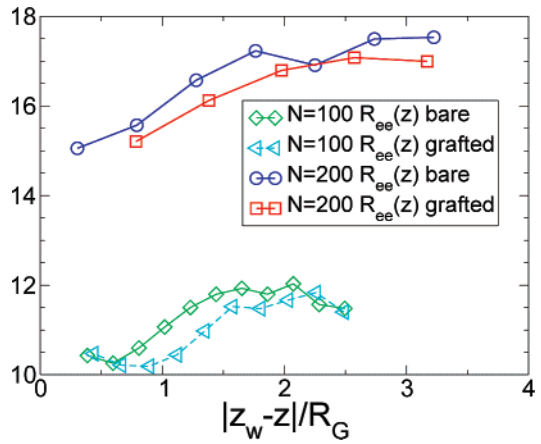

Figure 12. Local end-to-end distance for $N = 100$ and 200.

remains essentially constant throughout the boundary layer, while it decreases in the presence of a bare wall. In the case of a bare surface the decrease in the chains R_G results in less interpenetration diminishing the primitive paths. At the same time there is a slightly more pronounced decrease in the end-to-end distance for the system with grafted chains as discussed previously (Figure 3 and 12). The grafted chains, being on average more extended than the free chains provide more entanglements in the plane parallel to the wall for the chains close to the interface, thus keeping their path length constant regardless of the fact that the perpendicular size of the chains diminishes leading to less interpenetration in the direction perpendicular to the wall.

The additional entanglements due to the grafted chains can be interpreted in terms of local increase in the entanglement density as shown in Figure 13. The bulk entanglement length found for $N = 200$ ($N_e \approx 63$) is in agreement with the result of reference 13 for dense bead spring melts with flexible chains. In the case of $N < 200$ the numerical value of the bulk N_{pp} is lower than the N_e value for the melt as there are on average less than 2 entanglements per chain. N_{pp} has a smaller value near the grafted wall and a larger value near a bare surface, compared to the middle of the film. The relative variation in N_{pp} is meaningful and corresponds to a general trend in the entanglement density. To verify this assumption, we measure the local entanglement densities (entanglements per monomer) in the studied systems, defined as $(L_{pp}(z)/a_{pp}(z) - 1)/N = (N/N_{pp} - 1)/N$. The results are shown in Figure 13.

In a region that extends about one R_G from the surface, there is a depletion of entanglements for a bare wall, as qualitatively predicted in ref 8. A similar behavior was also observed in ref

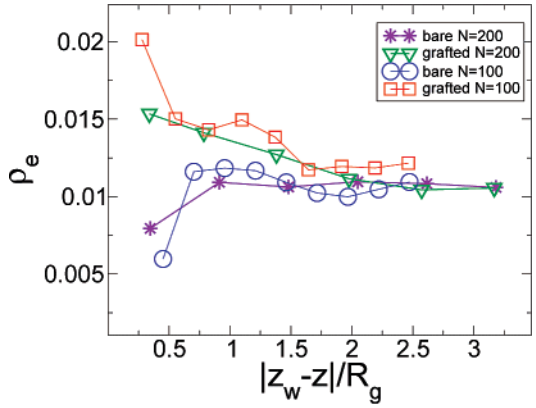

Figure 13. Local number of entanglements per monomer in the $N = 100$ and $N = 200$ systems. An increase in the entanglement density is seen for grafting wall, consistent with the measured variation in N_{pp} and N_e. A similar behavior is observed for $N = 50$.

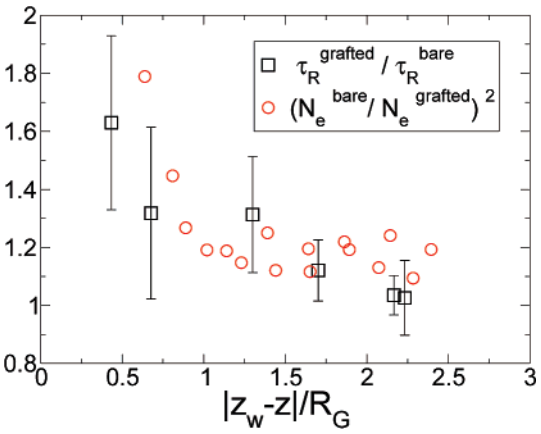

Figure 14. Comparison between the ratio of the local relaxation times (left term in eq 13) and the inverse square ratio of the local entanglement lengths (right term in eq 13) of the $N = 100$ systems with and without grafted chains.

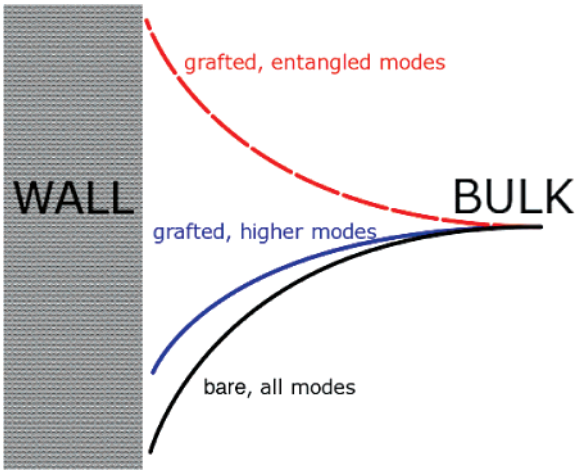

Figure 15. Schematic representation of the relative variation of the relaxation times of the modes of the polymer chains at the interface.

10. This effect was associated with smaller chain size in the z direction. It can be also understood knowing that chains in the immediate vicinity of the wall only have neighboring chains on one side and no chains to entangle with on the other side, so they have a smaller total number of entanglements. On the other hand, in presence of grafted chains the free chains near the surface do not feel its presence as far as entanglements are concerned as they still entangle with the chains grafted on the surface keeping a constant primitive path length. Moreover as the perpendicular dimensions of the free chains are reduced we end up with an interfacial region with higher density of entanglements. This difference in entanglement density explains the slowing down in the dynamics of the entangled modes. Moreover, a quantitative prediction can be established. Knowing from reptation theory that the relaxation of an entangled chain is proportional to $N \times ((N/N_e))^2$, the ratio between the relaxation times of two systems of equal chain length should be equal to the inverse square ratio of the entanglement lengths in the two cases, i.e.

$$\frac{\tau_R^{\text{grafted}}}{\tau_R^{\text{bare}}} = \left(\frac{N_e^{\text{bare}}}{N_e^{\text{grafted}}}\right)^2 \tag{13}$$

This relation provides a way to predict dynamics from a static equilibrium quantity in the melt. It is reasonably well verified in the interfacial layer of our $N = 100$ system, even if the melt is only weakly entangled at this chain length (see Figure 14).

V. Discussion and Conclusions

We presented here a study of the dynamic and static behavior for a polymer melt at the interface with a flat wall and a wall subject to surface treatment creating about 20% of chemisorbing sites on the surface. We find that the modifications in the dynamics due to the surface treatment depends on the level of entanglement of the melt. In the case of unentangled melts, the dynamics is accelerated compared to the bulk due to the surface. The grafted chains locally slow down the dynamics in the surface plane compared to systems without grafted chains, but the relaxation times are smaller than in the bulk and there is a local decrease in the integrated stress relaxation function as in the case of a bare wall. In the case of weakly entangled melts, the presence of the surface induces a decrease (∼20−40%) in the entanglement density in a range of about R_G from the surface. The presence of the grafted chains prevents this depletion of the entanglements and further reduces the entanglement length in the interfacial layer, in part due to the smaller chain dimensions. This leads to slower dynamics in the interfacial layer and a local increase of the relaxation times of the entangled modes near the surface. A summary of the dynamical behavior of the chains is given in Figure 15. The behavior of the relaxation times can be predicted by measuring the local entanglement length, following the expression given by reptation theory.

Our results on dynamics are obtained for chains that are only slightly above the entanglement threshold, but the primitive path analysis extends to chains further in the entangled regime. The results of the two methods are consistent, and if a contribution from the grafted chains is added, we can explain the observed moderate reinforcement in systems of $T \geq 2T_g$, where there can be no formation of glassy bridges.

We expect that these conclusions would hold for highly entangled melts. For longer chains the extension of the region where entanglement effects are enhanced by the grafting will be larger. It is likely that the motion of the chains perpendicular to the interface will be slowed down as well within this region, as entanglements will also hinder this type of motion.

A possible reason for the decrease in the entanglement density near a bare surface, measured with the standard primitive path algorithm, could be an increased number of self-entanglements and less interchain entanglements in the interfacial layer. This question will be discussed in detail in a future article using a primitive path algorithm preserving self-entanglements.[14] For the systems presented here, self-entanglements have a negligible

contribution, but their role seems to become important for chains of length $N > 500$.[21]

We note that the explanation of reinforcement by local variation of the entanglement length we proposed here is also relevant in a wider range of systems. We considered a surface with a certain number of infinitely attractive sites, but similar effects can be expected for a surface with a fraction of finitely attractive sites or a globally attractive surface. Thus, the slowing down of the adsorbed, slowest chains can be mediated by the entanglement network. This effect plays a role in the mechanical properties of nanocomposite polymer based materials for $T > T_g$ and low filler volume fraction with filler filler distance on the order of the chains R_G.[3]

Acknowledgment. Finally, we would like to thank Pr. Ralf Everaers for fruitful discussions concerning the primitive path analysis and the IDRIS for a grant of computer time.

References and Notes

(1) Payne, A. R. *J. Appl. Polym. Sci.* **1962**, *6*, 57.
(2) For a recent review, see: Oberdisse, J. *Soft Matter* **2006**, *2*, 29.
(3) Sternstein, S. S.; Zhu, A.-J. *Macromolecules* **2002**, *35*, 7262.
(4) Dalmas, F.; Chazeau, L.; Gauthier, C.; Cavaille, J. Y.; Dendievel, R. *Polymer* **2006**, *47*, 2802−2812.
(5) Berriot, J.; Montes, H.; Lequeux, F.; Long, D.; Sotta, P. *Europhys. Lett.* **2003**, *64*, 50.
(6) Baschnagel, J.; Varnik, F. *J. Phys.: Condens. Matter* **2005**, *17*, 851.
(7) Itagaki, H.; Nishimura, Y.; Sagisaka, E.; Grohens, Y. *Langmuir* **2006**, *22*, 742.
(8) Brown, H. R.; Russell, T. P. *Macromolecules* **1996**, *29*, 798.
(9) Oslanec, R.; Brown, H. R. *Macromolecules* **2003**, *36*, 5839.
(10) Meyer, H.; Kreer, T.; Cavallo, A.; Wittmer, J. P.; Baschnagel, J. To be published in *J. Phys. IV Fr.* **2006**.
(11) Wang, J.-S.; Binder, K. *J. Phys. (Paris)* **1991**, *1*, 1583.
(12) Kumar, S. K.; Vacatello, M.; Yoon, D. Y. *Macromolecules* **1990**, *23*, 2189.
(13) Everaers, R.; Sukumaran, S. K.; Grest, G. S.; Svaneborg, C.; Sivasubremanian, A.; Kremer, K. *Science* **2004**, *203*, 823.
(14) Sukumaran, S. K.; Grest, G. S.; Kremer, K.; Everaers, R. *J. Polym. Sci.* **2005**, 43, 917.
(15) Vladkov, M.; Barrat, J.-L. *Macromol. Theor. Simul.* **2006**, *15*, 252.
(16) Kremer, K.; Grest, G. S. *J. Chem. Phys.* **1990**, *92*, 5057.
(17) Flory, P. J. *Statistical Mechanics of Chain Molecules*; Interscience: New York, 1969.
(18) Nath, S. K.; Frischknecht, A. L.; Curro, J. G.; McCoy, J. D. *Macromolecules* **2005**, *38*, 8562.
(19) Smith, K. A.; Vladkov, M.; Barrat, J.-L. *Macromolecules* **2005**, *38*, 571.
(20) Huber, G.; Vilgis, T. A. *Eur. Phys. J. B* **1998**, *3*, 217.
(21) Meyer, H.; Vladkov, M.; Barrat, J.-L. Manuscript in preparation.
(22) S. J. Plimpton, *J. Comp. Phys.* **1995**, *117*, 1. LAMMPS web site: http://lammps.sandia.gov.

MA062607R